

7-2021

## Membrane inlet mass spectrometry method (REOX/MIMS) to measure $^{15}\text{N}$ -nitrate in isotope-enrichment experiments

Xianbiao Lin

Kaijun Lu

Amber K. Hardison  
*Virginia Institute of Marine Science*

et al

Follow this and additional works at: <https://scholarworks.wm.edu/vimsarticles>



Part of the [Geochemistry Commons](#)

---

### Recommended Citation

Lin, Xianbiao; Lu, Kaijun; Hardison, Amber K.; and et al, Membrane inlet mass spectrometry method (REOX/MIMS) to measure  $^{15}\text{N}$ -nitrate in isotope-enrichment experiments (2021). *Ecological Indicators*. doi: 10.1016/j.ecolind.2021.107639

This Article is brought to you for free and open access by the Virginia Institute of Marine Science at W&M ScholarWorks. It has been accepted for inclusion in VIMS Articles by an authorized administrator of W&M ScholarWorks. For more information, please contact [scholarworks@wm.edu](mailto:scholarworks@wm.edu).



# Membrane inlet mass spectrometry method (REOX/MIMS) to measure $^{15}\text{N}$ -nitrate in isotope-enrichment experiments

Xianbiao Lin <sup>a,b,c,e,1</sup>, Kaijun Lu <sup>b,1</sup>, Amber K. Hardison <sup>b,d</sup>, Zhanfei Liu <sup>b</sup>, Xin Xu <sup>b</sup>, Dengzhou Gao <sup>c</sup>, Jun Gong <sup>a,e,\*</sup>, Wayne S. Gardner <sup>b</sup>

<sup>a</sup> Laboratory of Microbial Ecology and Matter Cycles, School of Marine Sciences, Sun Yat-Sen University, Zhuhai 519082, China

<sup>b</sup> The University of Texas at Austin Marine Science Institute, 750 Channel View Drive, Port Aransas, TX 78373, USA

<sup>c</sup> School of Geographic Sciences, Key Laboratory of Geographic Information Science of the Ministry of Education, East China Normal University, Shanghai 200241, China

<sup>d</sup> Virginia Institute of Marine Sciences, College of William and Mary, Gloucester Point, VA 23062, USA

<sup>e</sup> Southern Laboratory of Ocean Science and Engineering (Guangdong, Zhuhai), Zhuhai 519000, China

## ARTICLE INFO

### Keywords:

REOX/MIMS

$^{15}\text{NO}_3^-$

Gross nitrification

Gross  $\text{NO}_3^-$  immobilization

Isotope dilution method

## ABSTRACT

Using  $^{15}\text{N}$  stable isotope as a tracer to quantify N transformation rates in isotope-enrichment experiments improves understanding of the N cycle in various ecosystems. However, measuring  $^{15}\text{N}$ -nitrate ( $^{15}\text{NO}_3^-$ ) in small volumes of water for these experiments is a major challenge due to the inconvenience of preparing samples by traditional techniques. We developed a “REOX/MIMS” method by applying membrane inlet mass spectrometry (MIMS) to determining  $^{15}\text{NO}_3^-$  concentrations in a small volumes of water from isotope-enrichment experiments after converting the dissolved inorganic N to  $\text{N}_2$ . The nitrates ( $\text{NO}_3^- + \text{NO}_2^-$ ) were reduced to  $\text{NH}_4^+$  with zinc powder, and the ammonium ( $\text{NH}_4^+$ ) was then oxidized to  $\text{N}_2$  by hypobromite iodine solution. The resulting  $^{29}\text{N}_2$  and  $^{30}\text{N}_2$  were measured via MIMS. This optimized protocol provides a sensitive ( $\sim 0.1 \mu\text{M}$ ) and precise (relative standard deviation = 0.1–4.37%) approach to quantify  $^{15}\text{NO}_3^-$  concentrations (0.1–500  $\mu\text{M}$ ) in water samples over a wide range of salinities (0–35‰) and in 2 M KCl solution with excellent calibration curves ( $R^2 \geq 0.9996$ ,  $p < 0.0001$ ). The method was combined with  $^{15}\text{NO}_3^-$  isotope-enrichment incubation experiments to measure gross nitrification and gross  $\text{NO}_3^-$  immobilization rates in various ecosystems. It was rapid, accurate, and cost-effective. Future applications of this efficient approach will inform scientists, modelers and decision makers about mechanisms, sources, fates, and effects of  $\text{NO}_3^-$  delivered to or produced in numerous aquatic and terrestrial ecosystems.

## 1. Introduction

Human activities have altered the global N cycle, with anthropogenic N inputs exceeding natural N fixation during the past several decades (Davidson, 2009; Galloway et al., 2008). Excessive reactive N in terrestrial and marine ecosystems from large applications of fertilizer has impacted the balance of the global N cycle and contributed to numerous eco-environmental problems, such as widespread eutrophication, hypoxia expansion, and increased harmful algal blooms (Cai et al., 2011; Deegan et al., 2012; Diaz and Rosenberg, 2008). A comprehensive evaluation of N transformation rates in both temporal and spatial scales is needed to assess N fate and to develop effective

means to control N pollution in affected ecosystems. Tracing the fate of added  $^{15}\text{N}$ -labeled compounds provides a useful tool to separate the production and consumption of the target N compound, and thereby calculate its gross production or consumption rates in environmental and laboratory samples (Blackburn, 1979; Caperon et al., 1979). Using  $^{15}\text{N}$  to quantify these rates increases understanding of N cycling in diverse ecosystems including both source-sink and process information.

Sediment slurry incubation methods have been applied widely in  $^{15}\text{N}$  studies, and can provide high resolution data of N transformation rates in spatial and temporal scales (Lin et al., 2017a, 2017b; Shan et al., 2016; Plummer et al., 2015; Wang et al., 2012; Trimmer and Nicholls, 2009). With sediment slurry incubation technique, numerous samples

\* Corresponding author at: Sun Yat-Sen University, School of Marine Sciences, Laboratory of Microbial Ecology and Matter Cycles, 402 Teaching Building, 2 Daxue Road, Tangjiawan Town, Zhuhai City, Guangdong Province 519082, China.

E-mail address: [gongj27@mail.sysu.edu.cn](mailto:gongj27@mail.sysu.edu.cn) (J. Gong).

<sup>1</sup> Xianbiao Lin and Kaijun Lu contributed equally to this work.

<https://doi.org/10.1016/j.ecolind.2021.107639>

Received 24 February 2021; Received in revised form 17 March 2021; Accepted 18 March 2021

Available online 30 March 2021

1470-160X/© 2021 The Author(s).

Published by Elsevier Ltd.

This is an open access article under the CC BY-NC-ND license

(<http://creativecommons.org/licenses/by-nc-nd/4.0/>).

can be acquired efficiently, providing detailed information on how different environmental parameters affect N transformation rates. Under this scenario, a high-throughput  $^{15}\text{N}$  method is needed to keep up with the efficiency of incubations. Traditional methods for quantifying stable N isotopes in different forms apply elemental analyzer-isotope ratio mass spectrometry (EA-IRMS) (Altabet et al., 2019) or GC/MS (Houben et al., 2010; Isobe et al., 2011; Stark and Hart, 1996) after converting the target N compound(s) to a gaseous N-species (usually  $\text{N}_2$  or  $\text{N}_2\text{O}$ ). These techniques are robust and reliable, but are labor-intensive, and thus not ideal for measuring high resolution N transformation rates.

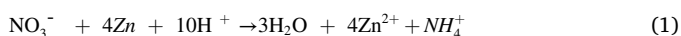
As noted above, sample pretreatment is an essential step in  $^{15}\text{NO}_3^-$  analysis. These pretreatments often involve chemical and microbial transformation of  $^{15}\text{NO}_3^-$  to other N-species, and subsequent diffusion techniques (Stark and Hart, 1996). The chemical conversions during pre-treatments are sometimes more convenient and precise than bacterial denitrifier reduction (Stevens and Laughlin, 1994), but involve toxic chemicals, such as cadmium, vanadium chloride ( $\text{VCl}_3$ ), hydrazine, and sodium hypobromite (Eschenbach et al., 2017, 2018; Houben et al., 2010; Stevens and Laughlin, 1994). A recent new one-step chemical method to convert  $\text{NO}_3^-$  to  $\text{N}_2\text{O}$  gas using Titanium chloride is simple, cost effective, and does not require toxic chemicals (Altabet et al., 2019), but requires ca. 24 h for titanium (Ti) the pretreatment process. Effective and high-throughput methods are needed to meet the demand of analyzing a large number of samples.

The more assessable membrane inlet mass spectrometry (MIMS) (Kana et al., 1994) and OXidation/MIMS (OX/MIMS) (Yin et al., 2014) technologies are used in increasing numbers of laboratories (Eschenbach et al., 2017, 2018). They provide sensitive, accurate, and cost-effective measurements of the  $^{15}\text{N}$  isotopic composition of  $\text{N}_2$  and ammonium ( $\text{NH}_4^+$ ), respectively, in water samples from isotope enrichment experiments. Here, we present an upgrade of the OX/MIMS method. The  $^{15}\text{NO}_3^-$  concentrations for isotope-enrichment experiments are determined in small volumes of samples (~15 mL) over a wide range of  $^{15}\text{NO}_3^-$  concentration (0.1–500  $\mu\text{M}$ ). This new REDuction-OXidation/MIMS (“REOX/MIMS”) approach extends the existing OX/MIMS method for measuring  $^{15}\text{NH}_4^+$  (Yin et al., 2014), to quantify  $^{15}\text{NO}_3^-$  concentration in  $^{15}\text{NO}_3^-$  isotope-enrichment experiments, and takes advantage of the unique features of MIMS analysis (high accuracy and precision, easy-to-operation, and support of high-throughput output) (Eschenbach et al., 2017; Groffman et al., 2006; Ketola et al., 2002; Richardson, 2001). The reduction of  $\text{NO}_3^-$  to  $\text{NH}_4^+$  was optimized by considering the effects of acidic condition, shaking frequency, quantity of zinc powder, reaction time, salinity, and temperature. The resulting  $^{15}\text{NH}_4^+$  was oxidized to  $\text{N}_2$  by hypobromite iodine solution (Ohyama and Kumazawa, 1981) and measured using OX/MIMS (Yin et al., 2014). We present preliminary results using this method to assess gross nitrification and  $\text{NO}_3^-$  immobilization in six ecosystems (grassland, forest, paddy, wetland, lacustrine, and estuarine environments) at Chongming Island in East China. The successful field trials demonstrate that this method provides a convenient tool to understand and predict N transformation rates in diverse natural environments.

## 2. Materials and methods

### 2.1. Reagents and experiment setup

The hypobromite iodine solution was prepared and stored at  $-20\text{ }^\circ\text{C}$  before conducting isotope-dilution experiments (Ohyama and Kumazawa, 1981; Yin et al., 2014). For analyses, 15 mL water samples fortified with  $^{15}\text{NO}_3^-$  were acidified with 75  $\mu\text{L}$  of 2 M sulfuric acid ( $\text{H}_2\text{SO}_4$ ). Nitrates (including the added  $^{15}\text{NO}_3^-$ ) were reduced to  $\text{NH}_4^+$  with zinc powder (Mallinckrodt, USA) in 50 mL centrifuge tubes. The reaction equation (Brown, 1921) is:



Water samples,  $\text{H}_2\text{SO}_4$  and zinc powder were mixed thoroughly for 30 min at room temperature in tubes using a platform shaker at 250 rpm. After mixing, the solutions were transferred into 12 mL gastight borosilicate vials (Labco Exetainer, High Wycombe, Buckinghamshire, UK). The vials were filled completely and sealed with silicon septa and screw caps to prevent leakage of solution and gas. To analyze the  $\text{NH}_4^+$ , excessive hypobromite iodine solution (0.2 mL) was injected into each sample vial to oxidize the  $^{15}\text{NH}_4^+$  to  $^{29}\text{N}_2$  and/or  $^{30}\text{N}_2$  (Yin et al., 2014). After oxidation, produced  $\text{N}_2$  gases were analyzed with MIMS (Hidden HPR-40, Hidden Analytical Ltd., Warrington, UK). The general procedure of the “REOX/MIMS” method to determine of  $^{15}\text{NO}_3^-$  in aqueous samples is shown in Fig. 1a.

For measurement, the aqueous sample was pumped at a rate of  $\sim 2.5\text{ mL min}^{-1}$  by a peristaltic pump (Minipuls 2, Gilson, Villiers le Bel, France; Fig. 1b P). It entered a stainless-steel capillary (i.d. 0.5 mm, length 1 m; Fig. 1b SC), held at  $25\text{ }^\circ\text{C}$  in a water bath (Fig. 1b T) to stabilize the sample temperature to within  $0.01\text{ }^\circ\text{C}$  (Ferrón et al., 2016). Before reaching the quadrupole mass analyzer (around  $1.33 \times 10^{-5}\text{ Pa}$ ; Fig. 1b Q), the dissolved gases were separated from the liquids by a membrane injector (Fig. 1b M) and the  $\text{H}_2\text{O}$  and  $\text{CO}_2$  were removed by a cryotrap ( $-110\text{ }^\circ\text{C}$ , liquid  $\text{N}_2$ , Fig. 1b C). Inside the quadrupole mass analyzer, dissolved gases were ionized using an oxide coated iridium filament to allow the selection of ionization energies (between 4 and 150 eV) and emission intensities (between 20 and 5000  $\mu\text{A}$ ). Once ionized, dissolved gases were separated by the quadrupole according to their mass to charge ratios ( $m/z$  ratios). Finally, the detection of dissolved gases is performed either by a secondary electron multiplier (Fig. 1b SEM).

### 2.2. $^{15}\text{N}$ standard evaluation

Three standard  $\text{Na}^{15}\text{NO}_3^-$  (99.4 atom%) solutions (5, 50, and 500  $\mu\text{M}$ ) were used to optimize several parameters of the proposed method (Method S1, Supporting Information). Three standard  $^{15}\text{NH}_4\text{Cl}$  (99.09 atom%) solutions (5, 50, and 500  $\mu\text{M}$ ) were prepared to calculate the  $^{15}\text{NO}_3^-$  reduction efficiency. The reduction efficiencies ( $R$ , %) were calculated with the following equation:

$$R = \frac{C_n}{C_a} \times 100\% \quad (2)$$

where  $C_n$  is the measured concentrations of  $^{15}\text{NH}_4^+$  after  $^{15}\text{NO}_3^-$  reduction, calculated from a standard OX/MIMS calibration curve (Yin et al., 2014);  $C_a$  is the respective concentrations of  $^{15}\text{NO}_3^-$  standards (5, 50, and 500  $\mu\text{M}$ ).

The detection limit and the applicability of REOX/MIMS for  $^{15}\text{NO}_3^-$  measurement in different matrices (in solutions with different salinity and in KCl solution) were evaluated. With optimized reaction conditions, the standards of  $\text{Na}^{15}\text{NO}_3^-$  were prepared with a concentration gradient of 0, 0.5, 1, 2, 5, 10, 15, 20, 50, 100, 200, 300, and 500  $\mu\text{M}$  at salinities of 5, 15, 35‰, and also in a 2 M KCl solution. Triplicate calibration-curve standards were prepared for each concentration. Standard solution (15 mL) was acidified with 75  $\mu\text{L}$  2 M  $\text{H}_2\text{SO}_4$  and  $\text{NO}_3^-$  was reduced to  $\text{NH}_4^+$  with 250 mg zinc powder in 50 mL centrifuge tubes. The tubes were mixed at 250 rpm for 30 min at room temperature. After incubation,  $^{15}\text{NH}_4^+$  was analyzed following the protocol shown in Fig. 1a.

### 2.3. Application of REOX/MIMS to field samples

The proposed REOX/MIMS method combined with the isotope dilution technique (Method S2, Supporting Information) was applied to measuring gross nitrification and  $\text{NO}_3^-$  immobilization rates in soil/sediment samples collected from different ecosystems in Chongming Island, Shanghai. Both the concentrations of total  $\text{NO}_3^-$  ( $^{14}\text{N} + ^{15}\text{N}$ ) and the atom% of  $^{15}\text{N}$  are required for isotope dilution experiments

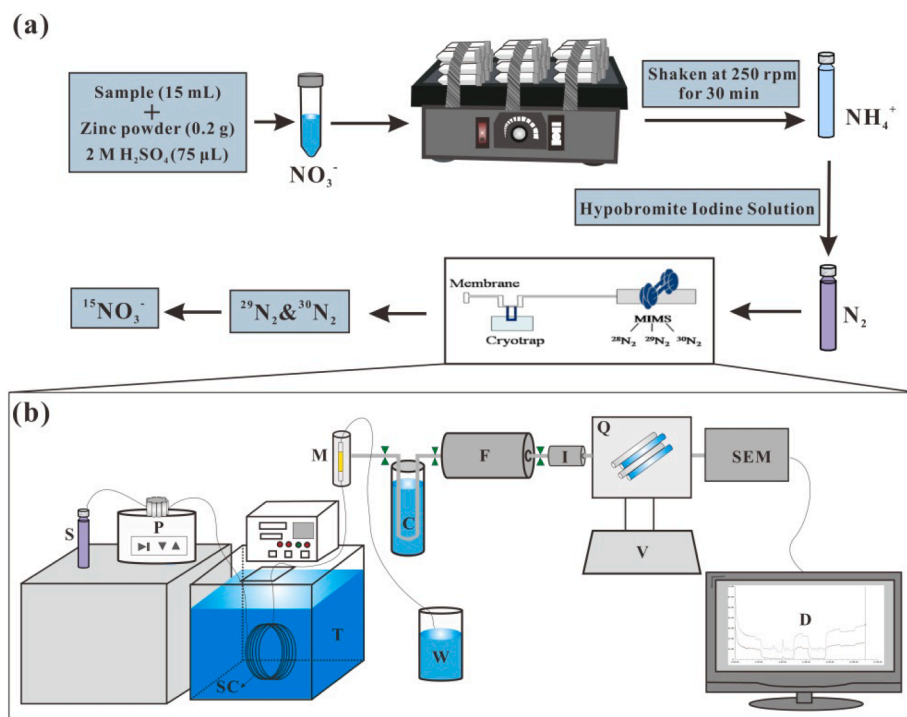


**Fig. 1.** The general procedure of the “REOX/MIMS” method for determination of  $^{15}\text{NO}_3^-$  in aqueous samples (a) and the schematic diagram of self-assembled membrane injection mass spectrometry system (b); The main components of this system are: sample vial (S), injection peristaltic pump (P), constant temperature water bath (T), stainless steel capillary (SC), membrane injector (M, including a gas-permeable silicone elastomer tube and a thick glass tubing), waste recovery bottle (W), cold trap (C), copper reduction furnace (F, containing a quartz tube with reduced copper wire), vacuum system (V), Ion source (I), quadrupole mass analyzer (Q), secondary electron multiplier (SEM), data processing system (D).

(Blackburn, 1979; Caperton et al., 1979; Chen et al., 2016). The total  $\text{NO}_3^-$  concentration was analyzed by a continuous-flow nutrient auto-analyzer (SAN Plus, Skalar Analytical B.V., the Netherlands), and the  $^{15}\text{NO}_3^-$  concentration was determined by REOX/MIMS under the optimized conditions. The  $^{15}\text{N}$  atom% was then determined based on the actual measurements. The gross nitrification rates and  $\text{NO}_3^-$  consumption rates were calculated following the isotope dilution equation (Barraclough et al., 1985; Bjarnason, 1988):

$$GNR = \frac{M_i - M_f}{t} \times \frac{\log(H_i M_f / H_f M_i)}{\log(M_i / M_f)} \quad (3)$$

$$GNC = \frac{M_i - M_f}{t} \times \frac{\log(H_i / H_f)}{\log(M_i / M_f)} \quad (4)$$

where  $GNR$  and  $GNC$  ( $\mu\text{g N g}^{-1} \text{d}^{-1}$ ) are the respective rates of gross nitrification and  $\text{NO}_3^-$  consumption;  $M_i$  and  $M_f$  ( $\mu\text{g N g}^{-1}$ ) are the respective concentrations of total  $\text{NO}_3^-$  in initial and final sediment/soil;  $H_i$  and  $H_f$  ( $\mu\text{g N g}^{-1}$ ) are the respective concentrations of  $^{15}\text{NO}_3^-$  in initial and final sediment/soil;  $t$  (d) is the incubation time. Since plants were excluded in our experiments,  $\text{NO}_3^-$  uptake by plants was assumed to be zero. Also,  $\text{NO}_3^-$  consumption through denitrification, anammox, and DNRA were considered to be negligible under aerobic conditions (Thamdrup and Dalsgaard, 2002; Zhao et al., 2015). Therefore, the gross  $\text{NO}_3^-$  immobilization rate was assumed equivalent to the gross  $\text{NO}_3^-$  consumption rate in aerobic environments.

### 3. Results and discussion

#### 3.1. Optimization conditions, accuracy and precision of REOX/MIMS

Based on a previous study (Carini et al., 2010) and our experiments, the effects of acidity, shaking frequency, zinc powder, reduction time, salinity, and temperature on the  $^{15}\text{NO}_3^-$  reduction were examined to optimize reaction conditions (Fig. 2). Results showed that the optimized conditions for 15 mL sample are 75  $\mu\text{L}$  2 M  $\text{H}_2\text{SO}_4$  and 250 mg zinc powder in 50 mL centrifuge tubes, and then mixed at 250 rpm for 30 min at room temperature (Fig. 2).

Under the optimized reaction conditions identified above, the REOX/MIMS calibration curves were prepared for aqueous samples containing different atom fractions of  $^{15}\text{NO}_3^-$  (0, 0.5, 1, 2, 5, 10, 15, 20, 50, 100, 200, 300, and 500  $\mu\text{M}$ ) at salinities of 0, 15, and 35‰, as well as in 2 M KCl solution. Regressions between the signal intensities of total  $^{15}\text{N}$  ( $10^{-9}$  Amps), and the concentrations of  $^{15}\text{NO}_3^-$  were linear below 20  $\mu\text{M}$  (Fig. 3a), and correlated significantly with salinity ( $R^2 = 0.9996$ , 0.9995, and 0.9992 for 0, 15, and 35‰, respectively,  $p < 0.0001$ ) and 2 M KCl solutions ( $R^2 = 0.999$ ,  $p < 0.0001$ ). When the concentration range was expanded to 500  $\mu\text{M}$ , the linearity remained strong, as indicated by high correlation coefficients at different salinities ( $R^2 = 0.9998$ , 0.9999, and 0.9997 for 0, 15, and 35‰, respectively,  $p < 0.0001$  for all) and 2 M KCl solutions ( $R^2 = 0.9996$ ,  $p < 0.0001$ ; Fig. 3b). Overall, the accuracy of REOX/MIMS ranged from 89.8% to 94.6%, with an average of  $92.4 \pm 1.2\%$ . A low relative standard deviation (RSD) was found at different  $^{15}\text{NO}_3^-$  concentrations (0.5–500  $\mu\text{M}$ ), varying from 0.1% to 4.37% with an average of  $1.49 \pm 0.87\%$ . Compared with existing methods (Eschenbach et al., 2017, 2018), our experimental data showed that REOX/MIMS had a wide detection range, with the lower limit as low as 0.1  $\mu\text{M}$  (calculated as twice the standard deviation of replicate blank samples (Tortell, 2005)), and the upper limit as high as 500  $\mu\text{M}$ , which accommodates most samples collected from isotope dilution experiments conducted in natural environments. Several methods (using GC-MS, IRMS and HPLC) can quantify the  $^{15}\text{NO}_3^-$  contents accurately in sea water and soil and sediment KCl extracts (Carini et al., 2010; Isobe et al., 2011; Preston et al., 1998). In a recent study, the SPIN-MIMS method determined  $^{15}\text{NH}_4^+$  and  $^{15}\text{NO}_3^-$  concentrations accurately in freshwater and soil extracts (Pennock et al., 1999). To compare with existing methods, REOX/MIMS were also tested for soil extracts. The high correlation coefficients at different salinities as well as in 2 M KCl solutions (Fig. 3) suggests that the method is affected minimally by salinity or KCl concentration ( $R^2 \geq 0.9996$ ,  $p < 0.0001$  for all). These results indicate that the REOX/MIMS method provides an accurate and precise approach to quantify  $^{15}\text{NO}_3^-$  concentrations over a concentration range of 0.1 to 500  $\mu\text{M}$  for water samples. However, the slightly different slopes for different salinities (Fig. 3) suggest that calibrations should be done with standard solutions having a similar salinity as the samples.

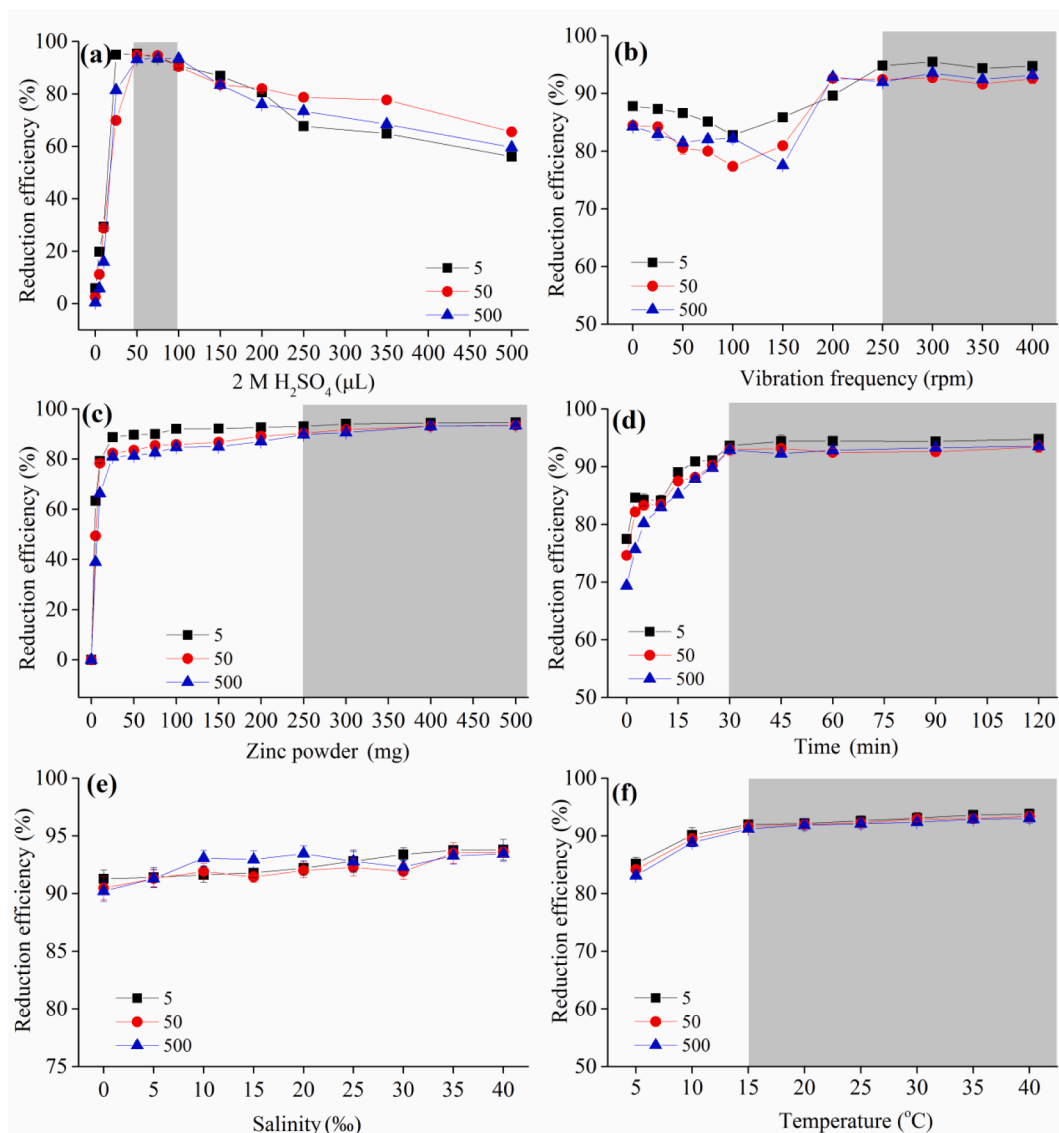


**Fig. 2.** Effects of the amount of  $\text{H}_2\text{SO}_4$  solution added (a), vibration frequency (b), zinc powder mass (c), reaction time (d), salinity (e), and incubation temperature (f) on  $^{15}\text{NO}_3^-$  reduction efficiency. Standard solutions with 5, 50, and 500  $\mu\text{M}$  of  $^{15}\text{NO}_3^-$  were used for all reactions. The grey areas indicate that the reduction rates have reached relatively stable and higher levels at corresponding conditions. Error bars represent standard deviations ( $n = 3$ ).

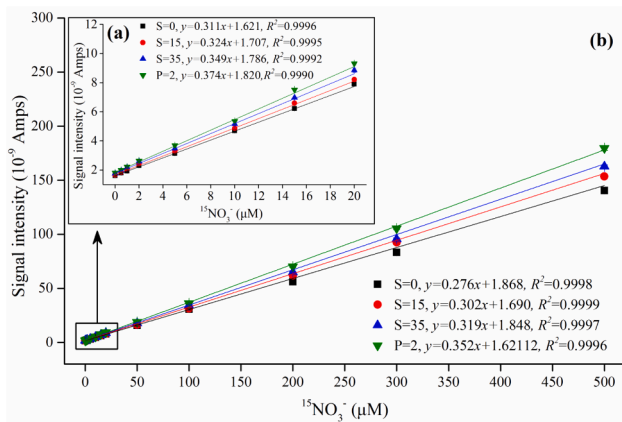


**Fig. 3.** Relationships of the known  $^{15}\text{NO}_3^-$  concentrations with measured signal intensities of total  $^{15}\text{N}$  ( $^{29}\text{N}_2 + 2 \times ^{30}\text{N}_2$ ) under optimal condition at salinity of 0, 15, and 35‰, as well as at solution of 2 M KCl. Vertical bars denote the standard errors ( $n = 3$ ). S and P represent salinity and 2 M KCl, respectively.

In addition to accurately measuring of  $^{15}\text{N}$  concentration, the correlation coefficient between the measured and expected  $^{15}\text{N}$  fraction was also high ( $R^2 = 0.9998$ ,  $p < 0.0001$ ) (Fig. 4a). The RSD of measured  $^{15}\text{N}$  fraction from the REOX/MIMS method was within an acceptable range (0.37–3.43%) at different  $^{15}\text{N}$  abundances and N concentrations, except for the 1 atom% standard at 10  $\mu\text{M}$  (RSD = 15.25%) (Fig. 4).

### 3.2. Field examination of gross nitrification and $\text{NO}_3^-$ immobilization rates

The gross nitrification rates ranged from 0.05 to 3.37  $\mu\text{g N g}^{-1} \text{d}^{-1}$  dry weight (grassland), 0.05 to 6.14  $\mu\text{g N g}^{-1} \text{d}^{-1}$  (forest), 0.07 to 3.07  $\mu\text{g N g}^{-1} \text{d}^{-1}$  (paddy), 0.02 to 3.95  $\mu\text{g N g}^{-1} \text{d}^{-1}$  (wetland), 0.03 to 1.20  $\mu\text{g N g}^{-1} \text{d}^{-1}$  (lacustrine), and 0.02 to 1.12  $\mu\text{g N g}^{-1} \text{d}^{-1}$  (estuarine soils/sediments), respectively (Fig. S1). The measured gross  $\text{NO}_3^-$  immobilization rates in grassland and forest soils varied from 0.01 to 5.94  $\mu\text{g N g}^{-1} \text{d}^{-1}$  and 0 to 10.07  $\mu\text{g N g}^{-1} \text{d}^{-1}$ , respectively (Fig. S1). Although deep soils/sediments contain ~33% of total N (Batjes, 1996) and 35–58% of total microbial biomass (Fierer et al., 2003; Schütz et al., 2010), the determined gross nitrification and  $\text{NO}_3^-$  immobilization rates

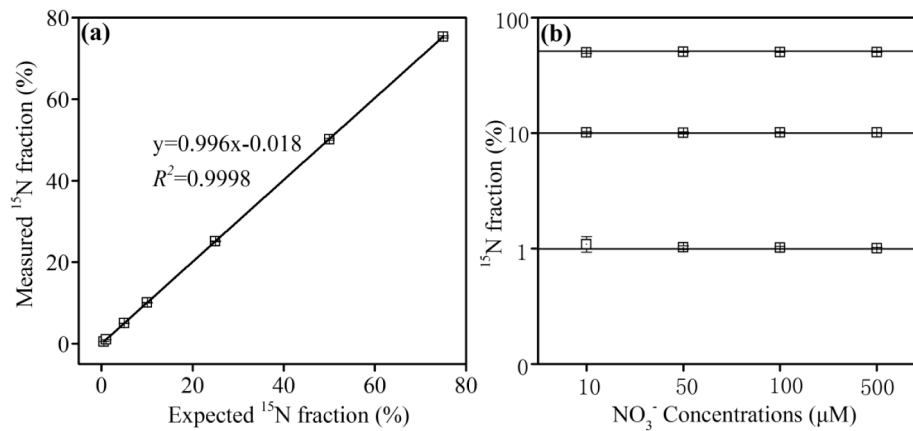


Fig. 4. (a) Relationships of the measured  $^{15}\text{N}$  fraction (0.5, 1, 5, 10, 25, 50, and 75%) with expected  $^{15}\text{N}$  fraction for standards at 500  $\mu\text{M}$ , (b)  $^{15}\text{N}$  abundances measured by at different  $\text{NO}_3^-$  concentrations ( $n = 3$ , mean and standard deviation).

in our study generally peaked in the top layer samples (0–5 cm) and declined greatly with depth (Fig. S1), a vertical pattern in coincidence with the depth gradients of oxygen and available substrate in soils/sediments (Altmann et al., 2003; Davidson et al., 1991; Wang et al., 2014). The rates for field samples of different ecosystems are comparable to existing records for other habitats across the world (Table S1, Supporting Information), indicating the proposed REOX-MIMS method is reliable.

Surface soils/sediments (0–5 cm) were selected and re-analyzed using two conventional methods to assess the comparative performance of REOX/MIMS. The results of gross nitrification and  $\text{NO}_3^-$  immobilization rates obtained using REOX/MIMS agree well with those obtained using IRMS (Finnigan MAT delta plus advantage) (Hojberg et al., 1994; Laughlin et al., 1994) or with a gas chromatograph equipped with a quadrupole-type mass spectrometer (GC-MS) (Isobe et al., 2011). The paired  $t$  test showed no statistical differences between these methods (Table 1). The precision of our method (RSD generally less than 5%) was also on a par with two conventional methods. These results demonstrated that REOX/MIMS is a practical technique to measure gross nitrification and  $\text{NO}_3^-$  immobilization rates accurately by isotope dilution in various ecosystems.

### 3.3. Evaluation of REOX/MIMS: advantages, disadvantages, and possible future applications

Over the last few decades, MIMS has been used increasingly to quantify the microbial N-transformation rates in isotope-enrichment experiments due to its high precision, rapid sample throughput,

Table 1

Comparison of GNR and GNI ( $\mu\text{g N g}^{-1} \text{d}^{-1}$ ) determined by three different methods in surface soils/sediments of our study area.

Sample (0–5 cm)	REOX/MIMS		GC-MS		IRMS	
	Mean	RSD %	Mean	RSD %	Mean	RSD %
Forest soils (GNR)	3.15	2.54	3.41	1.11	3.05	2.08
Forest soils (GNI)	6.74	0.82	6.84	0.72	6.45	1.03
Grassland soils (GNR)	2.15	4.13	2.38	1.35	2.11	2.24
Grassland soils (GNI)	4.25	1.29	4.54	1.66	4.11	1.99
Wetland sediments (GNR)	3.54	2.99	3.82	1.44	3.37	2.67
Paddy soils (GNR)	3.05	1.33	3.11	2.04	3.05	2.18
Lacustrine sediments (GNR)	1.24	3.80	1.33	2.71	1.08	4.55
Estuarine sediments (GNR)	0.55	4.60	0.61	3.28	0.49	6.27

Note: GNR and GNI mean gross nitrification and  $\text{NO}_3^-$  immobilization rates, respectively.

relatively wide dynamic ranges and cost-effectiveness (Crowe et al., 2012; Eyre et al., 2002; Hardison et al., 2015; Lin et al., 2017a; McCarthy and Gardner, 2003; McTigue et al., 2016; Yin et al., 2014). For instance, MIMS was applied to determining denitrification and anammox rates in sediments and water columns of aquatic ecosystems (Crowe et al., 2012; Eyre et al., 2002; Hardison et al., 2015; Lin et al., 2017b; McCarthy and Gardner, 2003; McTigue et al., 2016; Xie et al., 2020). The REOX/MIMS method present in this work provides a further development of the OX/MIMS method described by Yin et al. (2014). The OX/MIMS method to measure  $^{15}\text{NH}_4^+$  for isotope-enrichment experiments provides a convenient way to measure DNRA rates in sediments (Yin et al., 2014), and to determine N fixation, mineralization and immobilization with isotope tracer or dilution techniques in sediments of aquatic environments (Lin et al., 2016a, 2016b, 2017a; Richards and Friess, 2016). With this extension of the OX/MIMS method, all main N-transformation processes in the soils/sediments from various ecosystems (Fig. S1) can be quantified with MIMS methodology. This approach is convenient for investigating inland processes which affect the fate and effects of anthropogenic N from fertilizer use, and other industrial and municipal inputs into aquatic and terrestrial ecosystems (Galloway et al., 2008). Furthermore, REOX/MIMS can be modified further to determine  $\text{DO}^{15}\text{N}$  concentration using UV oxidation (Armstrong, 1968; Lu et al., 2020) and/or persulfate oxidation (Bronk et al., 2000). Determination of  $\text{DO}^{15}\text{N}$  concentration is important for controlled incubation experiments, which employ  $^{15}\text{N}$ -labeled substrate to track the fate and dynamics of DON in various ecosystems.

Our results show that REOX/MIMS accurately measures  $^{15}\text{N}$  abundances in  $^{15}\text{N}$ -enriched samples for  $^{15}\text{NO}_3^-$  at concentrations as low as 0.5  $\mu\text{M}$  and atom% as low as 1% regardless of the matrices (accuracy >89.81%, RSD < 5%, Fig. 4), resembling those of FT-IR (Kieber et al., 1998), IRMS (Laughlin et al., 1994) and R-CFMS methods (Russow, 1999) (Table S2, Supporting Information). Additionally, the comparison between REOX/MIMS and two traditional methods (IRMS and GCMS) for field samples shows good agreement for the measurement of gross nitrification and  $\text{NO}_3^-$  immobilization rates (Table 1). These traditional methods are more time-consuming and labor-intensive than our described method.

Another advantage of REOX/MIMS is its efficiency, which is critical for high-throughput analysis. Up to 50 samples can be processed simultaneously within one hour in a pre-treatment process (Fig. 1a). On a routine basis, approximately 5 min are required to analyze one sample by REOX/MIMS, compared with ca. 10–15 min for IRMS (Hojberg et al., 1994; Laughlin et al., 1994), GCMS (Isobe et al., 2011), and SPIN-MIMS (Eschenbach et al., 2017, 2018), and more than 40 min FT-IR/HPLC (Carini et al., 2010; Kieber et al., 1998) (Table S2, Supporting Information). The ability to handle a large quantity of samples make a high-

resolution measurement of N transformation rates possible.

$^{15}\text{NO}_3^-$  measurements by REOX/MIMS are routinely made with a sample volume of 15 mL. This volume is comparable to that required for the R-CFMS (Russow, 1999), GC-MS (Isobe et al., 2011), and AIRTS-HPLC (Carini et al., 2010) methods, but much smaller than the amount necessary for the IRMS (Hojberg et al., 1994; Laughlin et al., 1994) and FT-IR (Kieber et al., 1998) methods (Table S2, Supporting Information), but larger than the sample amount requirement (1.5 mL) for SPIN-MIMS (Eschenbach et al., 2018; Pennock et al., 1999). Note that measuring  $\text{N}_2$  as an analyte for the REOX/MIMS method remains a problem for  $^{15}\text{NO}_3^-$  abundance measurements in low concentration (i.e., less than 0.1  $\mu\text{M}$  in concentration and less than 1% in atom%) aqueous samples (Fig. 4). This result might explain the better sensitivity and accuracy of  $\text{NO}$  or  $\text{N}_2\text{O}$  as analytes at low  $\text{NO}_3^-$  concentrations and low  $^{15}\text{N}$  enrichments in previous studies (Eschenbach et al., 2018; Pennock et al., 1999). Thus, the REOX/MIMS is not the preferred method for trace-level enrichment or natural abundance  $^{15}\text{N}$  analysis. The methods reported by Liu et al. (2014), McIlvin and Altabet (2005), Sigman et al. (2001) and Stark and Hart (1996), provide more precise results at natural abundance levels. However, as noted above it can accurately determine  $^{15}\text{NO}_3^-$  concentrations and atom% from soil/sediment samples of N labeling studies despite a high atmospheric  $\text{N}_2$  background, and will be useful in  $^{15}\text{N}$  tracer studies to monitor time-course patterns in the future.

Overall, this work demonstrates that the REOX/MIMS method, involving the reduction of  $\text{NO}_3^-$  to  $\text{NH}_4^+$  by zinc powder and the subsequent transformation of the  $\text{NH}_4^+$  to  $\text{N}_2$  gas, provides a simple but robust approach to analyze samples from enrichment studies even at low concentrations and atom%.

#### 4. Conclusions

A new stream-lined method (REOX/MIMS) of determining  $^{15}\text{NO}_3^-$  concentrations for isotope-enrichment experiments via MIMS is presented. The REOX/MIMS method provides a low-cost, convenient, and accurate approach to quantify  $^{15}\text{NO}_3^-$  concentrations in water samples with a wide range of salinities ( $R^2 \geq 0.9997$ ,  $p < 0.0001$ ) and in a 2 M KCl solution ( $R^2 = 0.9996$ ,  $p < 0.0001$ ). Immediate advantages of this method include: (1) High accuracy (RSD =  $1.49 \pm 0.87\%$ ), (2) small sample volume requirement (15 mL), (3) simple and convenient handling, and (4) high-throughput (up to 12 samples can be measured per hour). This method is applicable in various ecosystems from lakes to forests. Importantly, like MIMS for  $^{15}\text{N}_2$  and OX/MIMS for  $^{15}\text{NH}_4^+$ , REOX/MIMS for  $^{15}\text{NO}_3^-$  offers the important advantage of direct measurements in the water, without evaporating or purifying the water from the samples. For example, by controlling the form of  $^{15}\text{N}$  added to the sample water for isotope-addition incubation experiments, one can determine changes in the  $^{15}\text{N}$  substrate or reaction product expected from adding the labeled compound to the water. Application of REOX/MIMS method should encourage kinetic experiments needed to provide comprehensive understanding of  $\text{NO}_3^-$  dynamics (e.g. sources and sinks) and thus contribute quantitatively to our understanding and modeling of N transformations, fate, and effects in numerous ecosystems affected by N dynamics on local, regional, and global scales.

#### CRedit authorship contribution statement

**Xianbiao Lin:** Data curation, Formal analysis, Funding acquisition, Investigation, Methodology, Project administration, Resources, Software, Supervision, Validation, Visualization, Writing - original draft, Writing - review & editing. **Kaijun Lu:** Data curation, Formal analysis, Writing - review & editing. **Amber K. Hardison:** Writing - review & editing. **Zhanfei Liu:** Writing - review & editing. **Xin Xu:** Formal analysis, Writing - review & editing. **Dengzhou Gao:** Formal analysis, Writing - review & editing. **Jun Gong:** Funding acquisition, Writing - review & editing. **Wayne S. Gardner:** Writing - review & editing.

#### Declaration of Competing Interest

The authors declare that they have no known competing financial interests or personal relationships that could have appeared to influence the work reported in this paper.

#### Acknowledgments

This work was jointly supported by the Marine S&T Fund of Shandong Province for Pilot National Laboratory for Marine Science and Technology (Qingdao) (No. 2018SDKJ0406-4), the National Natural Science Foundation of China (Nos. 42001088, 41976128), the Basic Research and Applied Basic Research of Guangdong Province of China (2019A1515110794), Project funded by China Postdoctoral Science Foundation (No. 2019M653151), and the Fundamental Research Funds for the Central Universities (No.19lgpy93 and No.181gzd07). We thank Yijie Zheng, Wenjing Li, and Ruyu Yan for much help and direction in analyzing samples, and also thank Guodong Song for much help in drawing the schematic diagram of self-assembled membrane injection mass spectrometry system.

#### Appendix A. Supplementary data

Optimization of reaction conditions and the standard calibration curve; Application of REOX/MIMS; Fig. S1; Table S1-2. Supplementary data to this article can be found online at <https://doi.org/10.1016/j.ecolind.2021.107639>.

#### References

- Altabet, M.A., Wassenaar, L.I., Douence, C., Roy, R., 2019. A Ti(III) reduction method for one-step conversion of seawater and freshwater nitrate into  $\text{N}_2\text{O}$  for stable isotopic analysis of  $^{15}\text{N}/^{14}\text{N}$ ,  $^{18}\text{O}/^{16}\text{O}$  and  $^{17}\text{O}/^{16}\text{O}$ . *Rapid Commun. Mass Spectrom.* 33 (15), 1227–1239. <https://doi.org/10.1002/rcm.v33.1510.1002/rcm.8454>.
- Altmann, D., Stief, P., Amann, R., de Beer, D., Schramm, A., 2003. In situ distribution and activity of nitrifying bacteria in freshwater sediment. *Environ. Microbiol.* 5 (9), 798–803. <https://doi.org/10.1046/j.1469-2920.2003.00469.x>.
- McIlvin, M.R., Altabet, M.A., 2005. Chemical conversion of nitrate and nitrite to nitrous oxide for nitrogen and oxygen isotopic analysis in freshwater and seawater. *Anal. Chem.* 77 (17), 5589–5595. <https://doi.org/10.1021/ac050528s10.1021/ac050528s.s001>.
- Armstrong, F.A.J.T., 1968. Photochemical combustion of organic matter in sea water, for nitrogen, phosphorus and carbon determination. *J. Mar. Biol. Assoc. U.K.* 48, 143–152. <https://doi.org/10.1017/S0025315400032483>.
- Barracough, D., Geens, E.L., Davies, G.P., Maggs, J.M., 1985. Fate of fertilizer nitrogen. *Eur. J. Soil Sci.* 36, 593–603. <https://doi.org/10.1111/j.1365-2389.1985.tb00361.x>.
- Batjes, N.H., 1996. Total carbon and nitrogen in the soils of the world. *Eur. J. Soil Sci.* 47, 151–163. <https://doi.org/10.1111/ejss.12115>.
- Bjarnason, S., 1988. Calculation of gross nitrogen immobilization and mineralization in soil. *Eur. J. Soil Sci.* 39, 393–406. <https://doi.org/10.1111/j.1365-2389.1988.tb01225.x>.
- Blackburn, T.H., 1979. Method for measuring rates of  $\text{NH}_4^+$  turnover in anoxic marine sediments, using a  $^{15}\text{N-NH}_4^+$  dilution technique. *Appl. Environ. Microb.* 37, 760–765. <https://doi.org/10.1128/AEM.37.4.760-765.1979>.
- Bronk, D.A., Lomas, M.W., Glibert, P.M., Schukert, K.J., Sanderson, M.P., 2000. Total dissolved nitrogen analysis: comparisons between the persulfate, UV and high temperature oxidation methods. *Mar. Chem.* 69 (1-2), 163–178. [https://doi.org/10.1016/S0304-4203\(99\)00103-6](https://doi.org/10.1016/S0304-4203(99)00103-6).
- Brown, J.G., 1921. The states of iron in nitric acid. *J. Phys. Chem.* 25 (6), 429–454. <https://doi.org/10.1021/j150213a001>.
- Cai, W.-J., Hu, X., Huang, W.-J., Murrell, M.C., Lehrter, J.C., Lohrenz, S.E., Chou, W.-C., Zhai, W., Hollibaugh, J.T., Wang, Y., Zhao, P., Guo, X., Gundersen, K., Dai, M., Gong, G.-C., 2011. Acidification of subsurface coastal waters enhanced by eutrophication. *Nat. Geosci.* 4 (11), 766–770. <https://doi.org/10.1038/ngeo1297>.
- Caperon, J., Schell, D., Hirota, J., Laws, E., 1979. Ammonium excretion rates in Kaneohe Bay, Hawaii, measured by a  $^{15}\text{N}$  isotope dilution technique. *Mar. Biol.* 54 (1), 33–40. <https://doi.org/10.1007/BF00387049>.
- Carini, S.A., McCarthy, M.J., Gardner, W.S., 2010. An isotope dilution method to measure nitrification rates in the northern Gulf of Mexico and other eutrophic waters. *Cont. Shelf Res.* 30 (17), 1795–1801. <https://doi.org/10.1016/j.csr.2010.08.001>.
- Chen, Z.Z., Zhang, J.B., Xiong, Z.Q., Pan, G.X., Mueller, C., 2016. Enhanced gross nitrogen transformation rates and nitrogen supply in paddy field under elevated atmospheric carbon dioxide and temperature. *Soil Biol. Biochem.* 94, 80–87. <https://doi.org/10.1016/j.soilbio.2015.11.025>.

- Crowe, S.A., Canfield, D.E., Mucci, A., Sundby, B., Maranger, R., 2012. Anammox, denitrification and fixed-nitrogen removal in sediments from the Lower St. Lawrence Estuary. *Biogeosciences* 9, 4309–4321. <https://doi.org/10.5194/bg-9-4309-2012>.
- Davidson, E.A., 2009. The contribution of manure and fertilizer nitrogen to atmospheric nitrous oxide since 1860. *Nat. Geosci.* 2 (9), 659–662. <https://doi.org/10.1038/ngeo608>.
- Davidson, E.A., Hart, S.C., Shanks, C.A., Firestone, M.K., 1991. Measuring gross nitrogen mineralization, and nitrification by  $^{15}\text{N}$  isotopic pool dilution in intact soil cores. *Eur. J. Soil Sci.* 42, 335–349. <https://doi.org/10.1111/j.1365-2389.1991.tb00413.x>.
- Deegan, L.A., Johnson, D.S., Warren, R.S., Peterson, B.J., Fleeger, J.W., Fagherazzi, S., Wollheim, W.M., 2012. Coastal eutrophication as a driver of salt marsh loss. *Nature* 490 (7420), 388–392.
- Diaz, R.J., Rosenberg, R., 2008. Spreading dead zones and consequences for marine ecosystems. *Science* 321 (5891), 926–929. <https://doi.org/10.1126/science.1156401>.
- Eschenbach, W., Lewicka-Szczepak, D., Stange, C.F., Dyckmans, J., Well, R., 2017. Measuring  $^{15}\text{N}$  abundance and concentration of aqueous nitrate, nitrite, and ammonium by membrane inlet quadrupole mass spectrometry. *Anal. Chem.* 89 (11), 6076–6081. <https://doi.org/10.1021/acs.analchem.7b00724>.
- Eschenbach, W., Well, R., Dyckmans, J., 2018. NO reduction to  $\text{N}_2\text{O}$  improves nitrate  $^{15}\text{N}$  abundance analysis by membrane inlet quadrupole mass spectrometry. *Anal. Chem.* 90 (19), 11216–11218. <https://doi.org/10.1021/acs.analchem.8b02956>.
- Eyre, B.D., Rysgaard, S., Dalsgaard, T., Christensen, P.B., 2002. Comparison of isotope pairing and  $\text{N}_2$ : Ar methods for measuring sediment denitrification—assumption, modifications, and implications. *Estuaries* 25 (6), 1077–1087. <https://doi.org/10.1007/BF02692205>.
- Ferrón, S., del Valle, D.A., Björkman, K.M., Quay, P.D., Church, M.J., Karl, D.M., 2016. Application of membrane inlet mass spectrometry to measure aquatic gross primary production by the  $^{18}\text{O}$  in vitro method. *Limnol. Oceanogr. Methods* 14 (9), 610–622. <https://doi.org/10.1002/lom3.v14.9>. <https://doi.org/10.1002/lom3.10116>.
- Fierer, N., Schimel, J.P., Holden, P.A., 2003. Variations in microbial community composition through two soil depth profiles. *Soil Biol. Biochem.* 35 (1), 167–176. [https://doi.org/10.1016/S0038-0717\(02\)00251-1](https://doi.org/10.1016/S0038-0717(02)00251-1).
- Galloway, J.N., Townsend, A.R., Erismann, J.W., Bekunda, M., Cai, Z., Freney, J.R., Martinelli, L.A., Seitzinger, S.P., Sutton, M.A., 2008. Transformation of the nitrogen cycle: Recent trends, questions, and potential solutions. *Science* 320 (5878), 889–892. <https://doi.org/10.1126/science.1136674>.
- Groffman, P.M., Altabet, M.A., Bohlke, J.K., Butterbachbahl, K., David, M.B., Firestone, M.K., et al., 2006. Methods for measuring denitrification: diverse approaches to a difficult problem. *Com. Appl.* 16, 2091–2122. [https://doi.org/10.1890/1051-0761\(2006\)016\[2091:MFMDDA\]2.0.CO;2](https://doi.org/10.1890/1051-0761(2006)016[2091:MFMDDA]2.0.CO;2).
- Hardison, A.K., Algar, C.K., Giblin, A.E., Rich, J.J., 2015. Influence of organic carbon and nitrate loading on partitioning between dissimilatory nitrate reduction to ammonium (DNRA) and  $\text{N}_2$  production. *Geochim. Cosmochim. Acta* 164, 146–160. <https://doi.org/10.1016/j.gca.2015.04.049>.
- Højberg, O., Johansen, H.S., Sørensen, J., 1994. Determination of  $^{15}\text{N}$  abundance in nanogram pools of  $\text{NO}_3$  and  $\text{NO}_2$  by denitrification bioassay and mass spectrometry. *Appl. Environ. Microb.* 60, 2467–2472. <https://doi.org/10.1128/AEM.60.7.2467-2472.1994>.
- Houben, E., Hamer, H.M., Luypaerts, A., De Preter, V., Evenepoel, P., Rutgeerts, P., Verbeke, K., 2010. Quantification of (15)N-nitrate in urine with gas chromatography combustion isotope ratio mass spectrometry to estimate endogenous NO production. *Anal. Chem.* 82 (2), 601–607. <https://doi.org/10.1021/ac9019208>.
- Isobe, K., Suwa, Y., Ikutani, J., Kuroiwa, M., Makita, T., Takebayashi, Y., et al., 2011. Analytical techniques for quantifying N-15/N-14 of nitrate, nitrite, total dissolved nitrogen and ammonium in environmental samples using a gas chromatograph equipped with a quadrupole mass spectrometer. *Microbes Environ.* 26, 46–53. <https://doi.org/10.1264/jsm2.ME10159>.
- Kana, T.M., Darkangelo, C., Hunt, M.D., Oldham, J.B., Bennett, G.E., Cornwell, J.C., 1994. Membrane inlet mass spectrometer for rapid high-precision determination of  $\text{N}_2$ ,  $\text{O}_2$ , and Ar in environmental water samples. *Anal. Chem.* 66 (23), 4166–4170. <https://doi.org/10.1021/ac00095a009>.
- Ketola, R.A., Kotiaho, T., Cisper, M.E., Allen, T.M., 2002. Environmental applications of membrane introduction mass spectrometry. *J. Mass Spectrom.* 37 (5), 457–476. <https://doi.org/10.1002/jms.v37:510>. <https://doi.org/10.1002/jms.327>.
- Kieber, R.J., Bullard, L., Seaton, P.J., 1998. Determination of  $^{15}\text{N}$  nitrate and nitrite in spiked natural waters. *Anal. Chem.* 70 (18), 3969–3973. <https://doi.org/10.1021/ac9802731>.
- Laughlin, R.J., Stevens, R.J., Zhuo, S., 1994. Determining nitrogen-15 in ammonium by producing nitrous oxide. *Soil Sci. Soc. Am. J.* 61, 462–465. <https://doi.org/10.2136/sssaj1997.03615995006100020013x>.
- Lin, X., Hou, L., Liu, M., Li, X., Yin, G., Zheng, Y., Deng, F., Vopel, K.C., 2016a. Gross nitrogen mineralization in surface sediments of the Yangtze Estuary. *PLoS ONE* 11 (3), e0151930. <https://doi.org/10.1371/journal.pone.0151930>.
- Lin, X., Hou, L., Liu, M., Li, X., Zheng, Y., Yin, G., Gao, J., Jiang, X., 2016b. Nitrogen mineralization and immobilization in sediments of the East China Sea: spatiotemporal variations and environmental implications. *J. Geophys. Res. Biogeosci.* 121 (11), 2842–2855. <https://doi.org/10.1002/2016JG003499>.
- Lin, X., Li, X., Gao, D., Liu, M., Cheng, L., 2017a. Ammonium production and removal in the sediments of Shanghai River networks: spatiotemporal variations, controlling factors, and environmental implications. *J. Geophys. Res. Biogeosci.* 122 (10), 2461–2478. <https://doi.org/10.1002/2017JG003769>.
- Lin, X., Liu, M., Hou, L., Gao, D., Li, X., Lu, K., Gao, J., 2017b. Nitrogen losses in sediments of the East China Sea: spatiotemporal variations, controlling factors and environmental implications. *J. Geophys. Res. Biogeosci.* 122 (10), 2699–2715. <https://doi.org/10.1002/2017JG004036>.
- Liu, D., Fang, Y., Tu, Y., Pan, Y., 2014. Chemical method for nitrogen isotopic analysis of ammonium at natural abundance. *Anal. Chem.* 86 (8), 3787–3792. <https://doi.org/10.1021/ac403756u>.
- Lu, K., Lin, X., Gardner, W.S., Liu, Z., 2020. A streamlined method to quantify the fates of  $^{15}\text{N}$  in seawater samples amended with  $^{15}\text{N}$ -labeled organic nitrogen. *Limnol. Oceanogr. Methods* 18 (2), 52–62. <https://doi.org/10.1002/lom3.10345>.
- McCarthy, M.J., Gardner, W.S., 2003. An application of membrane inlet mass spectrometry to measure denitrification in a recirculating mariculture system. *Aquaculture* 218 (1–4), 341–355. [https://doi.org/10.1016/S0044-8486\(02\)00581-1](https://doi.org/10.1016/S0044-8486(02)00581-1).
- McTigue, N.D., Gardner, W.S., Dunton, K.H., Hardison, A.K., 2016. Biotic and abiotic controls on co-occurring nitrogen cycling processes in shallow Arctic shelf sediments. *Nat. Commun.* 7, 13145. <https://doi.org/10.1038/ncomms13145>.
- Pennock, J.R., Boyer, J.N., Herrera-Silveira, J.A., Iversen, R.L., Whitedge, T., Mortazavi, B., et al., 1999. Nutrient behavior and phytoplankton production in Gulf of Mexico estuaries. *Biogeochem. Gulf of Mexico Estuaries* 109–162.
- Plummer, P., Tobias, C., Cady, D., 2015. Nitrogen reduction pathways in estuarine sediments: Influences of organic carbon and sulfide. *J. Geophys. Res. Biogeosci.* 120 (10), 1958–1972. <https://doi.org/10.1002/2015JG003057>.
- Preston, T., Zainal, K., Anderson, S., Bury, S.J., Slater, C., 1998. Isotope dilution analysis of combined nitrogen in natural waters: III. Nitrate and nitrite. *Rapid Commun. Mass Spectrom.* 12, 423–428. [https://doi.org/10.1002/\(SICI\)1097-0231\(19980430\)12:83.0.CO;2-2](https://doi.org/10.1002/(SICI)1097-0231(19980430)12:83.0.CO;2-2).
- Richards, D.R., Friess, D.A., 2016. Rates and drivers of mangrove deforestation in Southeast Asia, 2000–2012. *P. Natl. Acad. Sci. USA* 113 (2), 344–349. <https://doi.org/10.1073/pnas.1510272113>.
- Richardson, S.D., 2001. Mass spectrometry in environmental sciences. *Chem. Rev.* 101 (2), 211–254. <https://doi.org/10.1021/cr990090u>.
- Russow, R., 1999. Determination of  $^{15}\text{N}$  in  $^{15}\text{N}$ -enriched nitrite and nitrate in aqueous samples by reaction continuous flow quadrupole mass spectrometry. *Rapid Commun. Mass Spectrom.* RCM 13, 1334–1338. [https://doi.org/10.1002/\(SICI\)1097-0231\(19990715\)13:133.3.CO;2-3](https://doi.org/10.1002/(SICI)1097-0231(19990715)13:133.3.CO;2-3).
- Schütz, K., Kandler, E., Nagel, P., Scheu, S., Ruess, L., 2010. Functional microbial community response to nutrient pulses by artificial groundwater recharge practice in surface soils and subsoils. *FEMS Microbiol. Ecol.* 72, 445–455. <https://doi.org/10.1111/j.1574-6941.2010.00855.x>.
- Shan, J., Zhao, X., Sheng, R., Xia, Y., Qi, C., Quan, X., Wang, S., Wei, W., Yan, X., 2016. Dissimilatory nitrate reduction processes in typical Chinese paddy soils: rates, relative contributions and influencing factors. *Environ. Sci. Technol.* 50 (18), 9972–9980. <https://doi.org/10.1021/acs.est.6b01765>.
- Sigman, D.M., Casciotti, K.L., Andreani, M., Barford, C., Galanter, M., Böhlke, J.K., 2001. A bacterial method for the nitrogen isotopic analysis of nitrate in seawater and freshwater. *Anal. Chem.* 73 (17), 4145–4153. <https://doi.org/10.1021/ac010088e>.
- Stark, J.M., Hart, S.C., 1996. Diffusion technique for preparing salt solutions, kjeldahl digests, and persulfate digests for nitrogen-15 analysis. *Soil Sci. Soc. Am. J.* 60 (6), 1846–1855. <https://doi.org/10.2136/sssaj1996.03615995006000060033x>.
- Stevens, R.J., Laughlin, R.J., 1994. Determining nitrogen-15 in nitrite or nitrate by producing nitrous oxide. *Soil Sci. Soc. Am. J.* 58 (4), 1108–1116. <https://doi.org/10.2136/sssaj1994.03615995005800040015x>.
- Ohya, T., Kumazawa, K., 1981. A simple method for the preparation, purification and storage of  $^{15}\text{N}_2$  gas for biological nitrogen fixation studies. *Soil Sci. Plant Nutr.* 27 (2), 263–265. <https://doi.org/10.1080/00380768.1981.10431278>.
- Thamdrup, B., Dalsgaard, T., 2002. Production of  $\text{N}_2$  through anaerobic ammonium oxidation coupled to nitrate reduction in marine sediments. *Appl. Environ. Microb.* 68 (3), 1312–1318. <https://doi.org/10.1128/AEM.68.3.1312-1318.2002>.
- Tortell, P.D., 2005. Dissolved gas measurements in oceanic waters made by membrane inlet mass spectrometry. *Limnol. Oceanogr. Methods* 3 (1), 24–37. <https://doi.org/10.4319/lom.2005.3.24>.
- Trimmer, M., Nicholls, J.C., 2009. Production of nitrogen gas via anammox and denitrification in intact sediment cores along a continental shelf to slope transect in the North Atlantic. *Limnol. Oceanogr.* 54 (2), 577–589. <https://doi.org/10.4319/lo.2009.54.2.0577>.
- Wang, B., Zhao, J., Guo, Z., Ma, J., Xu, H., Jia, Z., 2014. Differential contributions of ammonia oxidizers and nitrite oxidizers to nitrification in four paddy soils. *ISME J.* 9 (5), 1062–1075. <https://doi.org/10.1038/ismej.2014.194>.
- Wang, S., Zhu, G., Peng, Y., Jetten, M.S.M., Yin, C., 2012. Anammox bacterial abundance, activity, and contribution in riparian sediments of the Pearl River estuary. *Environ. Sci. Technol.* 46 (16), 8834–8842. <https://doi.org/10.1021/es3017446>.
- Xie, C., Song, G., Liu, S., Tang, J., Zhang, G., 2020. Self-assembled membrane injection mass spectrometry (MIMS) system and its application on the study of dissimilatory nitrate reduction in sandy sediments. *Haiyang Xuebao* 42 (2), 22–29. <https://doi.org/10.3969/j.issn.0253-4193.2020.02.003>.
- Yin, G., Hou, L., Liu, M., Liu, Z., Gardner, W.S., 2014. A novel membrane inlet mass spectrometer method to measure  $^{15}\text{NH}_4^+$  for isotope-enrichment experiments in aquatic ecosystems. *Environ. Sci. Technol.* 48 (16), 9555–9562. <https://doi.org/10.1021/es501261s>.
- Zhao, W., Cai, Z., Xu, Z., 2015. Net and gross N transformation rates in subtropical forest soils under aerobic and anaerobic conditions. *J. Soil Sediment* 15 (1), 96–105. <https://doi.org/10.1007/s11368-014-1012-3>.